Available online at www.sciencedirect.com
ScienceDirect
Journal of Power Sources 173 (2007) 1–10
JOURNAL OF POWER SOURCES
www.elsevier.com/locate/jpowsour

Review

Alternative anode materials for solid oxide fuel cells

John B. Goodenough *, Yun-Hui Huang

Texas Materials Institute, ETC 9.102, 1 University Station, C2200, The University of Texas at Austin, Austin, TX 78712, USA

Received 11 June 2007; received in revised form 6 August 2007; accepted 8 August 2007
Available online 10 August 2007

Abstract

The electrolyte of a solid oxide fuel cell (SOFC) is an O^{2-}-ion conductor. The anode must oxidize the fuel with O^{2-} ions received from the electrolyte and it must deliver electrons of the fuel chemisorption reaction to a current collector. Cells operating on H_2 and CO generally use a porous Ni/electrolyte cermet that supports a thin, dense electrolyte. Ni acts as both the electronic conductor and the catalyst for splitting the H_2 bond; the oxidation of H_2 to H_2O occurs at the Ni/electrolyte/H_2 triple-phase boundary (TPB). The CO is oxidized at the oxide component of the cermet, which may be the electrolyte, yttria-stabilized zirconia, or a mixed oxide-ion/electron conductor (MIEC). The MIEC is commonly a Gd-doped ceria. The design and fabrication of these anodes are evaluated. Use of natural gas as the fuel requires another strategy, and MIECs are being explored for this application. The several constraints on these MIECs are outlined, and preliminary results of this on-going investigation are reviewed.

Keywords: Solid oxide fuel cells; Anode materials; Yttria-stabilized zirconia; Mixed oxide-ion/electron conductor

Contents

1. Introduction

Solid oxide fuel cells (SOFCs) convert the chemical energy of a fuel directly into electricity. Those presently under research/development and demonstration generally use as fuel the H_2 and CO gases of a reformed hydrocarbon. Although the SOFC operates at a high temperature, it has several significant applications because it promises cleaner, more efficient energy conversion than either a conventional power plant or lower temperature polymer-based fuel cells. Targeted applications include the bottoming cycle of an electric power plant, domestic heat and power units, and even electric vehicles [1–4]. The SOFC/gas turbine (GT) hybrid system has been recognized to offer efficient electricity generation, reaching net conversion efficiencies as high as 70% [5–7]. What has hindered the entrance of the SOFC into the market place is cost of construction and the lifetime of operation at a high temperature with duty demands requiring frequent temperature cycling. In this review, we consider the problems encountered in developing the anode, an electrode at which the fuel is oxidized and elec-

* Corresponding author. Tel.: +1 512 471 1646; fax: +1 512 471 7681.
E-mail address: jgoodenough@mail.utexas.edu (J.B. Goodenough).

0378-7753/$ – see front matter © 2007 Elsevier B.V. All rights reserved.
doi:10.1016/j.jpowsour.2007.08.011

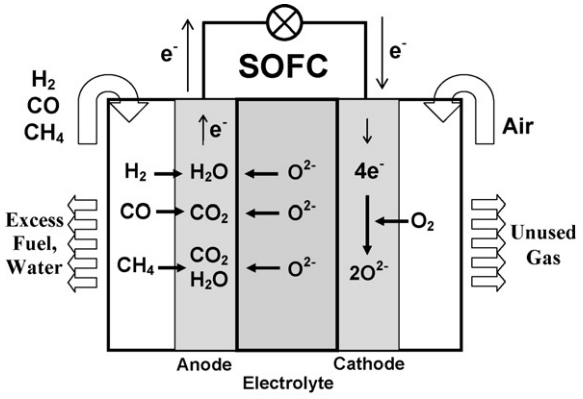

Fig. 1. Schematic of a solid oxide fuel cell (SOFC).

trons of the oxidation reaction are delivered to the external circuit.

The SOFC, represented schematically in Fig. 1, is an electrochemical device with a solid oxide-ion conductor as the electrolyte separating two electrodes, an anode and a cathode. In operation, the cathode acts as a catalyst for the reduction of oxygen, *i.e.* $O_2 + 4e^- = 2O^{2-}$, with electrons received from outside the cell; it also delivers the O^{2-} ions to the electrolyte. The function of the electrolyte is to block electron flow from the anode to the cathode inside the cell and to transport the O^{2-} ions from the cathode to the anode where they oxidize the fuel:

$$H_2 + O^{2-} = H_2O + 2e^- \quad (1)$$

$$CO + O^{2-} = CO_2 + 2e^- \quad (2)$$

$$CH_4 + 4O^{2-} = CO_2 + 2H_2O + 8e^- \quad (3)$$

are the overall oxidation reactions of most immediate interest. For the anode reaction to proceed, hydrogen and hydrocarbon fuels must be chemisorbed and dissociated onto the anode surface while CO from reformed hydrocarbon is nondissociatively adsorbed on the anode surface. The constituents must be brought into contact with the O^{2-} ions of the electrolyte; also, the electrons from the chemisorption reaction must be delivered to the external circuit where they perform work on their way to the cathode. The anode must also be able to exhaust the oxidation products to the atmosphere. Moreover, because the oxide-ion conductivity, σ_O, of the electrolyte is much smaller than the electronic conductivity, σ_e, of the electrodes and the external circuit and because the electronic and ionic currents must be matched during charge and discharge, the electrolyte is a thin (10–30 μm thick if operated below 800 °C), oxygen-deficient oxide of large area in order to reduce the internal cell resistance when operating at lower temperatures. For operation below 800 °C, the thin ceramic electrolyte must be supported on one of the electrodes, and the anode is normally chosen as the support.

The SOFC is not a heat engine; therefore, its efficiency is not limited by the Carnot cycle. Nevertheless, it is subject to internal losses that limit its efficiency, especially when operated at lower temperatures. The chemical reactions occurring at the electrodes and the O^{2-}-ion conductivity, σ_O, of the electrolyte are all activated, which means that the losses in a SOFC increase exponentially with decreasing temperature. Therefore, existing SOFCs having yttria-stabilized zirconia (YSZ) as the electrolyte operate at a $T_{OP} \approx 1000$ °C. Such SOFCs are generally of the electrolyte-supported geometry with 150 μm thickness if operated at $T_{OP} = 1000$ °C, but lower temperature operation with stabilized zirconia requires an electrolyte thickness of 10–30 μm and therefore an anode-supported geometry. Reduction of T_{OP} to below 800 °C would simplify manufacture, lower the cost of operation, and extend the life of the SOFC. Therefore, alternative materials having lower activation energies for O^{2-}-ion transport and for the catalytic chemical reactions at the electrode surfaces are high-priority research targets.

Fuels for SOFCs can range from hydrogen and CO to hydrocarbons to gasified coal. Most SOFCs can work well with fairly pure hydrogen and CO. Currently, hydrogen and CO are widely produced from hydrocarbons via reforming. CO is a main component of reformed hydrocarbons (reaction (9)). It is more practical to produce electricity directly from the hydrocarbon fuels. Natural gas that contains methane with small amounts of other hydrocarbons is very economic and popular for most stationary SOFC systems. Low-cost and readily available natural gas is preferred for SOFCs, as it would provide a cheaper, more convenient means of generating electricity. A SOFC operating on a liquid hydrocarbon would allow an even wider use of the SOFC, *e.g.* recharging batteries in an electric vehicle. Therefore, there is a strong incentive to develop anodes that can operate on methane, the principal component of natural gas, and on a gasified liquid fuel. Since natural gas and oil-derived liquid fuels contain sulfur as an impurity, the anodes must be sulfur-tolerant, *i.e.* immune from poisoning by sulfur of the catalytic sites at which the fuel is dissociatively chemisorbed, unless the sulfur is removed from the feed gas. Moreover, the electrochemical oxidation of CO at the surface of an oxide anode must be fast enough to prevent formation of coke deposits that block further reaction. In the case of methane, for example, the reaction

$$CH_4 + 3O^{2-} = CO + 2H_2O + 6e^- \quad (4)$$

at an oxide electrode surface is followed by (2) and the competing reaction

$$2CO = C + CO_2 \quad (5)$$

which results in C–C bond formation. On nickel, dissociative chemisorption is followed by spillover of hydrogen at the triple-phase boundary to an oxide, electrolyte or mixed oxide-ion/electronic conductor, to form H_2O in the reaction

$$CH_4 + 2O^{2-} = C + 2H_2O + 4e^- \quad (5')$$

and C–C bond formation on the nickel leads to coke build-up. If reaction (2) is faster than reaction (5) on an oxide anode, the electrode surface may remain free of coke build-up. Addition of some O_2 to the feed gas can also provide the reaction

$$2CO + O_2 = 2CO_2 \quad (6)$$

and on nickel

$$C + O_2 = CO_2 \quad (6')$$

to compete with reaction (5), but at the expense of the electrochemical reaction (2). Removal of CO from the surface by water in the reactions

$$CO + H_2O = CO_2 + H_2 \quad (7)$$

$$H_2 + O^{2-} = H_2O + 2e^- \quad (8)$$

is accompanied by the reformer reaction

$$CH_4 + H_2O = CO + 3H_2 \quad (9)$$

These reactions may arise from the water of reaction (4) or by adding steam to the feed gas. In the latter case, the endothermic steam-reforming reaction occurs near the outer surface of the anode whereas in the former case the endothermic reaction absorbs heat from the exothermic electrochemical conversion of H_2 into water and electricity thereby preventing creation of a large temperature gradient across the electrode.

In recent years, there have been several excellent reviews on the development or challenge of SOFC anode materials [8–14]. For example, McIntosh and Gorte [12] aimed at operating SOFC directly on hydrocarbon fuels and on anode materials that are compatible with direct hydrocarbon utilization; Tao and Irvine [13] reviewed the development of alternative SOFC anodes with fluorite, rutile, tungsten bronze, pyrochlore, perovskite and spinel structures. In this paper, we first point out the constraints on any design of an anode for the SOFC and discuss the status of the anodes used today in fuel cells operating on H_2 and CO. We then review on-going attempts either to build a reformer function into the anode or to find a sulfur-tolerant material that can catalyze oxidation of a hydrocarbon without formation of coke that blocks the anode function. We focus on the recent development on alternative anode materials, especially the double perovskites $Sr_2Mg_{1-x}Mn_xMoO_{6-\delta}$ that exhibit a superior single-cell performance in H_2 and CH_4 and an excellent tolerance to sulfur.

2. Constraints

There are five basic requirements that an anode must satisfy:

(1) *Catalytic activity*. Oxidation of hydrogen and hydrocarbons begins with a chemisorption and dissociation at the surface of the anode. The anode must facilitate this reaction with whatever fuel is to be used. This dissociative chemisorption needs to be followed by a reaction of the products of the dissociation with O^{2-} ions from the electrolyte, a step that may involve either transport of products to the electrolyte or of O^{2-} ions to the products. If a metal catalyst is used, the dissociation products must be transferred to the electrolyte, and the reaction with O^{2-} ions takes place near a linear triple-phase boundary (TPB) consisting of metal catalyst, oxide electrolyte, and fuel. In this case, chemisorption on the metal catalyst involves electron transfer from the fuel to the conduction band of the metal catalyst, which must subsequently transport these electrons to a current collector. However, if a mixed oxide-ion/electronic conductor (MIEC) is used as a catalytic anode, O^{2-} ions are transported to the anode surface from the electrolyte and both steps of the fuel-oxidation reaction occur on the surface of the MIEC anode. In this case, chemisorption involves transfer of an electron from the fuel to a mixed-valent redox couple of the MIEC; these electrons are transferred within the redox couple to either the catalytic metal of a cermet or directly to the current collector.

An imperative is that the catalytic activity remains high over a long life. This imperative requires that the anode is not poisoned by impurities in the feed gas or by carbonaceous residues if a hydrocarbon fuel is used; it also requires retention of the electronic pathways from the reaction sites to the current collector. Sulfur is a constituent of hydrocarbon fuels, and its removal is necessary as it poisons most catalysts. The more sulfur-tolerant the anode, the lower are the requirements for sulfur removal from the feed gas. Where Ni is used as the catalyst for H_2 dissociation, failure of the Ni to wet adequately the oxide surface results in Ni particulates that only contact one another through narrow necks. An imperative in this case is prevention of oxidation of the Ni to NiO during temperature cycling as the process of oxidation–reduction on cycling tends to brake the electrical contact between nickelate particles that is required for transporting the electrons of the chemisorption reaction to the current collector.

(2) *Electronic conductivity*. Electrons from the chemical reaction at the anode surface must be transported to the external circuit. Since the electrolyte has a large surface area, a metallic-screen current collector is used to reduce the distance electrons must travel in the anode itself; the electrons are transported long distances to the external circuit by the current collector. Nevertheless, resistive losses within the anode must be minimized by having a catalytic anode that is a good electronic conductor. If the anode acts as a support for the thin ceramic electrolyte, the electrons must travel a longer distance in the anode to reach the current collector, which requires a higher electronic conductivity of the catalytic anode material.

(3) *Thermal compatibility*. Since a SOFC is cycled between room temperature and T_{OP}, the thermal expansion of the anode must be matched to that of the electrolyte with which it makes chemical contact and, preferably, also to that of the current collector with which it makes physical contact.

(4) *Chemical stability*. The anode must be chemically stable at T_{OP} not only in the reducing atmosphere at the anode, but also with respect to the electrolyte and the current collector with which it makes contact. Interface phases that block electron transfer from the anode to the current collector or O^{2-}-ion transport from the electrolyte to the anode must not be formed over time under operating conditions. Moreover, if the anode is used to support the thin ceramic electrolyte, it must be chemically stable relative to the electrolyte under the conditions of sintering the electrolyte into a dense ceramic membrane.

(5) *Porosity*. Since the gaseous fuel must make contact with the TPB of the anode or with the surface of the MIEC over as large an area as is feasible, the anode must be fabricated as a porous structure that retains its physical shape over time

under operating conditions and the current collector must not cover the entire anode surface.

3. Ni/YSZ cermets: H_2 oxidation

Since the anode operates in a reducing atmosphere, metallic catalysts are candidate materials. Comparison of the electrochemical activities of Mn, Fe, Co, Ni, Ru, and Pt showed that Ni has the highest activity for H_2 reduction [15]. Pure nickel has a melting point of 1453 °C, a thermal expansion coefficient $\alpha = 13.3 \times 10^{-6}\,K^{-1}$ that is higher than the $\alpha \approx 10.5 \times 10^{-6}\,K^{-1}$ of a YSZ electrolyte, and a $\sigma_e \approx 2 \times 10^4\,S\,cm^{-1}$ at 1000 °C. Preparation of a NiO/YSZ cermet from fine NiO and YSZ particles has four important benefits [16,17]:

(1) The thermal expansion of the cermet may be better matched to that of the YSZ electrolyte.
(2) Reduction of the NiO in a wet hydrogen or fuel atmosphere creates a porous YSZ structure with metallic nickel particles on the surface of the pores. With a proper fabrication process, a strong YSZ framework contains an internal porous space percolating in 3D with contacting Ni particulates partially on the surface of this space also percolating in 3D. This configuration introduces a long TPB for the catalytic reaction and provides electronic conduction from the TPB to the current collector.
(3) Coarsening of the nickel film at T_{OP} that would break the conductive pathways for the electrons is inhibited [18–20].
(4) Ni and YSZ are essentially immiscible in each other and non-reactive over a wide temperature range, which simplifies synthesis of a Ni/YSZ cermet.

Therefore, the Ni/YSZ cermet anode was initially used for SOFCs; these SOFCs operate at a $T_{OP} \geq 800$ °C in pure H_2. The performance of a Ni/YSZ cermet anode depends critically on the microstructure of the porous YSZ framework and the distribution of the nickel on the surface of the percolating inner space. This dependence and the requirement that the structure remain stable over long periods at T_{OP} and many temperature cycles makes the efficacy of a Ni/YSZ anode critically dependent on fabrication procedures.

Conventional Ni/YSZ anodes may either support the electrolyte or be supported by the electrolyte. Present-day demonstration SOFCs operating below 800 °C use the anode to support the thin electrolyte and the cathode. Commercial NiO and YSZ fine powders are coarsened by heat treatment to give desired particle sizes and size distribution. The powders are then homogenized by mechanical mixing, pressed with or without a green electrolyte layer (or, if electrolyte supported, formed into an ink that is applied to the electrolyte), then sintered in air and finally annealed in wet H_2 or fuel to reduce the NiO to metallic nickel to form a porous Ni/YSZ anode. Initially, the green state contains a uniform distribution of NiO and YSZ particles. After sintering at 1400 °C in air, significant growth of both the NiO and YSZ particles occurs with some increase in porosity. Reduction of the NiO to Ni reduces the volume of this phase by 25%, thus greatly increasing the porosity and penetrating the pores with particles of metallic Ni. Electrode performance depends not only on the sizes of the YSZ and NiO starting particles, but also on the ratio of the particle sizes. For $(Y_2O_3)_{0.08}(ZrO_2)_{0.92}$ = 8YSZ, Murakami et al. [21] found their best performance with 8YSZ and NiO particles of size 0.5 μm and 2.5 μm, respectively, having the 8YSZ/NiO size ratio of ca. 0.2.

To achieve the YSZ–YSZ bonding and the NiO–NiO particle contacts necessary to achieve a stable 3D YSZ framework with a percolating porous space as well as good bonding to the YSZ electrolyte, it is necessary to sinter the composite at a high temperature, *e.g.* 1400 °C. These high temperatures also contribute to realization of a Ni-particulate necklace that percolates over the 3D internal porous surface [22]. However, sintering at high temperatures increases stresses at the anode–electrolyte interface due to mismatch of their thermal expansions; these stresses may lead to a fracture of the electrolyte that is initiated by cracks growing in the cermet [23,24].

The fraction of NiO in the cermet required for forming a percolating Ni necklace on the internal porous surface, and therefore for obtaining a good cermet electronic conductivity, is about 0.3–0.5. This fraction depends on the morphology of the YSZ framework, which is why the performance of the Ni/YSZ anode depends not only on the fraction of NiO in the cermet, but also on the particle sizes and the size ratio of the starting NiO and YSZ particles.

In order to improve the powder morphology and homogeneity of the starting NiO and YSZ powders obtained conventionally, several alternative synthetic routes have been investigated [25–38]. Selection of the best synthetic route depends on factors such as reproducibility, cost, and ease of scale-up.

Degradation over time of the performance of a Ni/YSZ anode operating on pure H_2 as the fuel is due to microstructural changes; the predominant change is the agglomeration and coarsening of the Ni phase as a result of the poor wettability of YSZ by nickel [39–42]. Sintering of pure Ni, which may occur at 1000 °C in H_2, leads to the formation of isolated islands and consequent loss of electrical connection to the current collector. Suppression of agglomeration and sintering of metallic nickel depends on optimization of the Ni/YSZ cermet microstructure [43]. Nevertheless, operation at high current densities and fuel utilization can cause agglomeration of the Ni even in optimized cermet structures [44]. Moreover, it is important to prevent reoxidation of the Ni on system shut down; the volume changes associated with repeated oxidation of Ni to NiO and reduction back to Ni on thermal cycling can break the connection between Ni particulates and weaken the mechanical strength of the porous YSZ framework [45].

Instead of co-firing a mixture of NiO and YSZ particles followed by reduction of the NiO to Ni, Craciun et al. [46] have obtained a comparable anode performance by impregnating a porous YSZ coating with an aqueous solution of Ni. The advantage of impregnation is that it allows the introduction of other conductors such as Cu and/or other catalysts. For example, impregnating a standard Ni/YSZ cermet with Ru as catalyst improved a cell power density by 33% [47].

4. Ni/YSZ cermets: CH_4 and syngas oxidation

The production of electricity from CH_4 is accomplished either by the complete oxidation of CH_4 or by reformation of the CH_4 to syngas before it is fed to the fuel cell. The complete oxidation of methane involves reactions (4) and (2) supplemented by reactions (7) and (8). In order to avoid the complication and expense of a separate reformer, attempts have been made to incorporate reaction (7) into the anode by combining steam with the CH_4 feed gas, but reaction (7) is always accompanied by reaction (9). It was found necessary to have a steam/carbon ratio of 2 or higher to prevent coke build-up on the Ni; this ratio proves to be too great to be practical [48]. On the other hand, under conditions of high current and low concentration (4–9%) of dry CH_4, no carbon build-up on the Ni occurs [49,50], especially for $T_{OP} \leq 700\,^{\circ}C$ [51–56]. Under these conditions, the water of reaction (4) reacts with the CH_4 feed gas as well as the adsorbed CO in reactions (7)–(9) to eliminate coke build-up in the anode. In a laboratory experiment, a direct methane SOFC with a YSZ electrolyte supported by a Ni/YSZ cermet anode has been reported to exhibit power densities as high as $0.52\,W\,cm^{-2}$ at 700 °C and $1.27\,W\,cm^{-2}$ at 800 °C in 4–8% CH_4 in Ar [55]. On the other hand, Lin et al. [57] noted that coke build-up on a Ni/YSZ cermet normally occurs primarily at the outer surface of the anode. They reasoned that the water of reactions (4) and (8) escapes from the anode surface before reaction (7) can occur. Therefore, they had the ingenious idea of adding a chemically inert, porous outer layer to the anode that acts as a diffusion barrier for the fuel gas so as to reduce the concentration of methane and increase the concentration of product H_2O throughout the anode. With a tubular SOFC design, they have achieved an equivalent ratio $O_2/CH_4 \approx 1.2$ within the anode to obtain at $T_{OP} = 750\,^{\circ}C$ an output power of $\approx 0.7\,W\,cm^{-2}$ at a $V \approx 0.4\,V$ [58]. This system also produces a high rate of syngas production.

Sulfur contamination in any hydrocarbon fuel is a problem for Ni-based anodes; they are poisoned by H_2S levels as low as 0.05 ppm at 800 °C, improving only slightly with increasing temperature [59]. Nevertheless, within a certain H_2S concentration level, the sulfur loss by sulfur poisoning is reversible upon removal of the sulfur source, which is viewed as evidence that the sulfur is physisorbed on the Ni [60,61].

5. Ni/RDC

Ceria doped with a rare earth or Y (RDC) has the same oxygen-deficient fluorite structure as YSZ, and these oxides become mixed oxide-ion/electronic conductors (MIECs) in the reducing atmosphere at the anode [62]. Moreover, the Ce^{4+}/Ce^{3+} redox couple has a low enough energy to be catalytically active for CO and hydrocarbon oxidation [63–65]. Therefore, Ni/RDC cermets are preferred if syngas is used as the fuel. Hirabayashi et al. [66] suggested that the surface of the perovskite electrolyte $BaCe_{0.76}Y_{0.20}Pr_{0.04}O_{3-\delta}$ may become the anode on reduction of the ceria under reducing gas conditions. This material is a proton conductor rather than an oxide-ion conductor at low temperatures; it loses water to become an MIEC with only mobile oxide-ions at T_{OP}. H_2 and, without carbon formation, hydrocarbons with more than one carbon/molecule gave a moderate cell performance at 800 °C; the catalytic activity for CH_4 was poor on the surface of this oxide. The availability of O^{2-} ions over the ceria surface enhances reactions (2) and (4), and Ni/RDC anodes have been reported to be effective in preventing coke build-up with CH_4 fuels [67,68]. For example, Gd-doped ceria (GDC), like $Ce_{0.6}Gd_{0.4}O_{1.8}$, is recognized to have the ability to suppress coke build-up; Marina et al. [68] and Livermore et al. [69] have reported a high activity to methane oxidation without carbon deposition with a Ni/GDC cermet anode. The performance of the Ni/RDC anodes can be further improved by dispersing uniformly trace amounts of noble-metal catalysts like Ru or Pd, especially at lower operating temperatures [70,71].

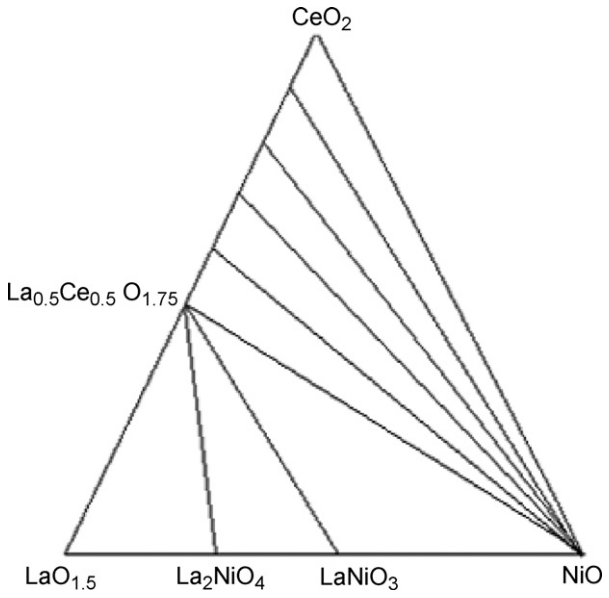

Fig. 2. Simplified phase diagram of the $LaO_{1.5}$–CeO_2–NiO system.

Chemical reaction at the anode/electrolyte interface can lead to interface phases that block O^{2-}-ion transport from the electrolyte to the anode. For example, GDC and YSZ react during sintering at 1200 °C to form a Gd-rich phase with O^{2-}-ion conductivity two orders of magnitude lower than that of YSZ at 800 °C [72,73]. In this case, a thin buffer layer of $Ce_{0.43}Zr_{0.43}Gd_{0.10}Y_{0.04}O_{1.93}$ between the anode and the electrolyte blocks the chemical reaction [74]. However, the Ni of a Ni/GDC anode was also found to inhibit reactivity between the YSZ and the ceria [73]. The perovskite electrolyte $La_{0.9}Sr_{0.1}Ga_{0.8}Mg_{0.2}O_{2.85}$ (LSGM) reacts with NiO and with Sm-doped ceria (SDC) of a Ni/SDC anode to form $LaNiO_3$, $LaSrGa_3O_7$, and $LaSrGaO_4$, all of which block O^{2-}-ion transport. The solution in this case was to introduce a $La_{0.6}Ce_{0.4}O_{1.7}$ (LDC) buffer layer having a La activity equal to that of the LSGM [75–79]. The phase relationships in the $LaO_{1.5}$–CeO_2–NiO system are illustrated in Fig. 2, which were confirmed experimentally [76]. No reaction products were found between CeO_2 and NiO. With a 200-μm-thick LSGM as the electrolyte and LDC as the buffer layer, a porous composite anode of Ni and

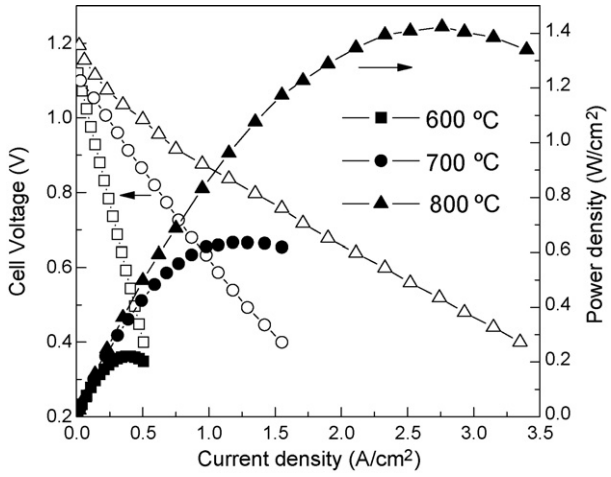

Fig. 3. Cell voltage, power density as a function of current density at various temperatures. The cell consists of air, Pt + SCF/LSGM/LDC/LDC + Ni, dry H_2 with 200-μm-thick LSGM electrolyte, $SrCo_{0.8}Fe_{0.2}O_3$ (SCF) cathode coated with sputtered Pt.

La-doped ceria exhibited a power density as high as 1.4 W cm^{-2} at 800 °C in H_2, as shown in Fig. 3 [77].

GDC works well as an electrolyte for an intermediate-temperature SOFC [80,81]. $Ce_{0.9}Gd_{0.1}O_{1.95}$ has an oxide-ion conductivity of 10^{-2} S cm^{-1} at 500 °C, and the Gd^{3+} ion is the preferred dopant compared to Sm^{3+} and Y^{3+} at this temperature [81]. Zha et al. [82] have co-pressed a Ni/GDC anode supporting a 20-μm-thick GDC electrolyte; the Ni of the anode was introduced by a solution-impregnation technique. A SOFC fabricated with this technique reached, at 600 °C with humidified H_2, CH_4, and C_3H_8, peak power densities of 0.60, 0.52, and 0.43 W cm^{-2}, respectively.

6. MIECs

Since carbon formation on Ni is a problem and since the RDCs are MIECs having some catalytic activity for oxidation of hydrocarbons, Gorte and co-workers [83–87] have replaced the Ni by impregnating ceria with Cu. In these anodes, Cu only provides electronic conductivity; the ceria, which becomes an MIEC in the reducing atmosphere at the anode, acts as the oxidation catalyst. Reaction (5′) does not occur on Cu, and the availability of O^{2-} on the surface of the ceria enhances reactions (2) and (7) over reaction (5) so as to suppress coke formation. A $Cu/CeO_2/YSZ$ composite anode has shown activity for direct electrochemical oxidation of a variety of dry hydrocarbon gases without degradation from carbon deposition. Compared with Ni/YSZ, a $Cu/CeO_2/YSZ$ anode exhibits a substantially better performance with carbonaceous fuels, especially with CO and syngas fuel [83,88]. However, in these anodes the YSZ and RDC portions must make good contact for O^{2-} transport across the interface [89]. To improve the catalytic activity of the Cu-impregnated composite anodes, McIntosh et al. [90] have systematically investigated the effect of dispersing Pt, Pd, and Rh into the pores with the Cu. P_{max} for operation on CH_4 was increased by a factor 10 over that obtained on a $Cu/CeO_2/YSZ$ anode without a noble metal. Putna et al. [91] have demonstrated that addition of Rh to a Cu/SDC anode improved significantly the cell performance in CH_4. Alternatively, the catalytic activity has been enhanced by replacing Cu with an alloy, *e.g.* Cu–Ni [92]. An $Fe_xCo_{0.5-x}Ni_{0.5}/Sm_{0.2}Ce_{0.8}O_{1.9}$ cermet anode showed a very low interfacial resistance to give a cell with a high P_{max} [93].

Importantly, the ceria-based anodes with Cu exhibit a high tolerance to sulfur poisoning. A $Cu/CeO_2/YSZ$ anode operating on H_2 fuel at 800 °C showed no degradation on introducing H_2S up to 450 ppm [94].

Baidya et al. [95] have shown that $Ce_{0.84}Ti_{0.15}Pt_{0.01}O_{2-\delta}$ crystallizes in the fluorite structure, has an enhanced reducibility compared to CeO_2, and shows a high catalytic activity for partial oxidation of hydrocarbons. This material, with or without Pt, has yet to be tested as the anode of a SOFC.

Since the RDCs are tolerant to sulfur and the ability of an RDC to replenish O^{2-} ions to its surface prevents coke build-up, the next logical step is to explore for other oxides that are MIECs in the reducing atmosphere at the anode and are catalytically more active than ceria for the oxidation of hydrocarbons. The perovskite structure readily accepts oxygen vacancies, and mixed-valent transition-metal perovskites are electronic conductors. Therefore, the $AMO_{3-\delta}$ perovskites containing a transition-metal M atom in the octahedral sites and a combination of rare-earth and alkaline-earth metals in the larger A sites is an attractive option. However, there are at least five constraints on this option:

1. Retention of electronic conductivity requires that the active redox couple on the M atom remain only partially reduced in the atmosphere at the anode, *i.e.* that the perovskite remains mixed-valent.
2. The active redox couple must have a low enough energy to accept electrons from H_2 or hydrocarbon fuel in order to induce its dissociative chemisorption on the oxide surface.
3. Catalytic activity requires an easy release of oxidized products from the surface as well as rapid replenishment of O^{2-} ions to the surface.
4. The oxygen vacancies that allow for O^{2-}-ion conduction must not be ordered at T_{OP}.
5. The thermal expansion must be compatible with that of the electrolyte.

The first two requirements narrow the acceptable energy range of the active redox couple. The third constraint requires that the cations, particularly the M atoms, have comparable energies in sixfold and fivefold or fourfold oxygen coordination. The fourth constraint may not be too stringent for $T_{OP} \geq 700$ °C provided the first is maintained, but retention of a mixed valence on the M atoms under operating conditions may require special atmosphere control to avoid a large thermal expansion due to reduction/oxidation on thermal cycling.

$La_{0.9}Sr_{0.1}Ga_{0.8}Mg_{0.2}O_{2.85}$ (LSGM) is an excellent O^{2-}-ion conductor; both Ga^{3+} and Mg^{2+} are stable in either tetrahedral or octahedral coordination as also is Mn^{2+}. Therefore, substitution of Mg by Mn in LSGMn has been explored as a possible anode

[96–100] since Mn^{2+} is stable in a reducing atmosphere. However, the Mn^{3+} concentration appears to be too small in the anode atmosphere for a competitive performance. This problem is less severe in the perovskite system $(La_{1-x}Sr_x)_{0.9}Cr_{0.5}Mn_{0.5}O_{3-\delta}$ explored by Tao and Irvine [101–103]. For a cell with a 0.3-mm-thick YSZ electrolyte supported by this anode and a porous $La_{0.8}Sr_{0.2}MnO_3$ cathode, the maximum power densities were 0.47 W cm^{-2} and 0.2 W cm^{-2} for wet H_2 and CH_4 at 900 °C, respectively [102]. Wan et al. [104] have shown that the addition of impregnated Cu and Pt to increase, respectively, the electronic conductivity and the catalytic activity raises these P_{max} values. However, these oxides aged and are poisoned by small amounts of sulfur in the fuel.

Aguilar et al. [105] have shown that H_2S is oxidized by the mixed-valent $La_{1-x}Sr_xVO_{3-\delta}$ (LSV) perovskite in the reaction

$$3O_s^{2-} + H_2S = SO_2 + H_2O \quad (10)$$

which makes a SOFC with an LSV anode tolerant to 10% H_2S in H_2, but the P_{max} at 1000 °C was not competitive. Reaction (10) appears to be selectively preferred over reaction with H_2. Zha et al. [106] have shown that the pyrochlore $Gd_2Ti_{1.4}Mo_{0.6}O_{7-\delta}$ can also operate on 10% H_2S in H_2 without poisoning by sulfur; reaction (10) is also operative on this MIEC.

Among the numerous other perovskite systems that have been explored, those containing Ti continue to attract attention because Ti remains mixed-valent Ti^{4+}/Ti^{3+} in the reducing atmosphere at the anode and this redox couple is stable enough in an oxide to accept electrons from a hydrocarbon or H_2 in a chemisorption dissociation reaction. Moreover, the Ti^{4+} ion accepts square-pyramidal oxygen coordination to allow removal of oxygen from the surface. But in order to sustain the fuel-oxidation reaction, the perovskite must also be a good oxide-ion conductor. Whereas most MIEC perovskites support oxide-ion conduction via oxygen vacancies, the $La_{1-x}Sr_xTiO_{3+\delta}$ perovskites are oxygen-rich; they accommodate the extra oxygen by introducing LaO (0 0 1) planes inserted between perovskite blocks. As a result, there are few mobile oxygen vacancies in the perovskite blocks. Nevertheless, these titanates have a high electronic conductivity, are stable in reducing conditions, and resist sulfur poisoning [107–110]. For $\delta < 1.167$, these extended defects become disordered and truncated, the perovskite is more easily reduced, and the oxide-ion conductivity, σ_O, increases. Nevertheless, σ_O remains too low to sustain a high rate of catalytic fuel oxidation because the Ti atoms prefer octahedral coordination in the bulk. To alleviate this situation, Ruiz-Morales et al. [111] introduced Mn and Ga; the Mn^{2+} and Ga^{3+} ions are stable in octahedral and tetrahedral oxygen coordination, which can facilitate oxygen-vacancy transfer. Single-phase $La_4Sr_8Ti_{11}Mn_{0.5}Ga_{0.5}O_{37.5}$ was prepared in air. In the reducing atmosphere at the anode, the Mn^{3+} is reduced to Mn^{2+} and some Ti^{4+} are reduced to Ti^{3+} to give good electronic conductivity on the Ti subarray. Moreover, oxygen vacancies are introduced into the perovskite blocks to give a high enough σ_O to sustain the catalytic fuel reduction reaction at a reasonable rate by replenishment of the O^{2-} ions on the surface. This material demonstrates impressive fuel-cell performance on wet hydrogen and is active for methane oxidation with open-circuit voltages in excess of 1.2 V at high temperatures. Fu et al. [112] have reported a similar performance with $La_{0.4}Sr_{0.6}Ti_{1-x}Mn_xO_{3-\delta}$. Vashook et al. [113] have suggested overlaying a film of $La_{0.1}Ca_{0.9}Ti_{0.9}Ru_{0.1}O_{3-\delta}$ on a $La_{0.1}Ca_{0.9}TiO_{3-\delta}$ anode to improve the catalytic activity.

The rate of the catalytic reaction at the surface of an anode may not be limited by the rate of diffusion of O^{2-} ions to the surface, but by the rate of chemisorption. Therefore, numerous studies have been directed to identification of catalytic additives to the surface. The need for a further acceleration of electocatalysis for the oxidation of CH_4 is made apparent by the lower P_{max} values with CH_4 versus H_2 as fuel. Ruthenium is an excellent catalyst for methane steam reforming. However, its use is limited by cost and by evaporation of RuO_x at high T_{OP}. Nevertheless, Sauvet et al. [114] have emphasized that the insertion of Ru into a perovskite can stabilize against RuO_x evaporation.

The double perovskite Sr_2FeMoO_6 is a ferromagnetic metal; Mössbauer data [115] show it has a mixed Fe^{3+}/Fe^{2+} valence and NMR [116] that it has a mixed Mo(VI)/Mo(V) valence, which means that the Mo(VI)/Mo(V) redox band overlaps the Fe^{3+}/Fe^{2+} couple. Therefore, since the Fe^{3+}/Fe^{2+} couple is at a high enough energy that even in a reducing atmosphere it is not possible to reduce all the Fe^{3+} ions completely to Fe^{2+} in $Fe_{1-\delta}O$, the Mo(VI)/Mo(V) redox couple can be expected to remain mixed-valent in the reducing atmosphere at the anode. Moreover, the ability of Mo(VI) and Mo(V) to form molybdyl ions allows a sixfold-coordinated Mo(VI) to accept an electron while losing an oxide ligand; this ability is the basis of the catalytic activity of the $(PMo_{12}O_{40})^{3-}$ Keggin ion to partially oxidize acrolein to acrylic acid [117]. However, removal of an O^{2-} ion from the surface of Sr_2FeMoO_6 is accompanied by stabilization of the Fe^{3+}/Fe^{2+} couple, and any additional lowering of the oxygen coordination at the iron atoms makes them susceptible to complete reduction to metallic iron. Therefore, if the oxide-ion conductivity of the MIEC is not great enough to keep the surface replenished with O^{2-} ions, metallic iron forms over time at the surface of the anode to degrade performance. On the other hand, if it is possible to replace the Fe by an M^{2+} cation that has a comparable preference for octahedral and tetrahedral coordination, the σ_O of the double perovskite will be enhanced and the loss of surface oxygen would not cause reduction of the M^{2+} ion to the metal. Since a mixed-valent Mo(VI)/Mo(V) redox band provides good electronic conductivity even where this band does not overlap a redox couple on the counter cations, replacement of Fe by $M = Mn_{1-x}Mg_x$ is a promising choice. The electronic conductivity of ceramic bars of $Sr_2Mg_{1-x}Mn_xMoO_{6-\delta}$ (SMMO) had a $\sigma_O \approx 10$ S cm^{-1} at 800 °C in H_2 and CH_4; and the system gives an excellent anode performance in both H_2 and CH_4 as well as moderate sulfur tolerance [118,119].

Fig. 4 shows cell voltage and power density as a function of current density at different temperatures for single cells with typical anodes of $Sr_2MgMoO_{6-\delta}$ in H_2, H_2 containing 5% H_2S, and CH_4. In these experiments a thin LDC buffer layer on 300-μm-thick LSGM was used as electrolyte; $SrCo_{0.8}Fe_{0.2}O_{3-\delta}$ was the cathode. For $Sr_2MgMoO_{6-\delta}$, a $P_{max} = 0.84$ W cm^{-2} at 800 °C and 0.45 W cm^{-2} at 700 °C in H_2

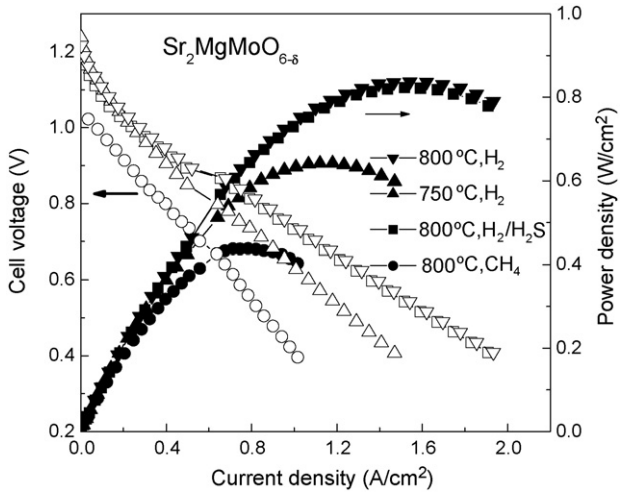

Fig. 4. Cell voltage, power density as a function of current density for single fuel cells with anodes of $Sr_2MgMoO_{6-\delta}$ in different fuels H_2, H_2/H_2S, CH_4. The open symbols represent the cell voltages while the closed symbols represent the power densities.

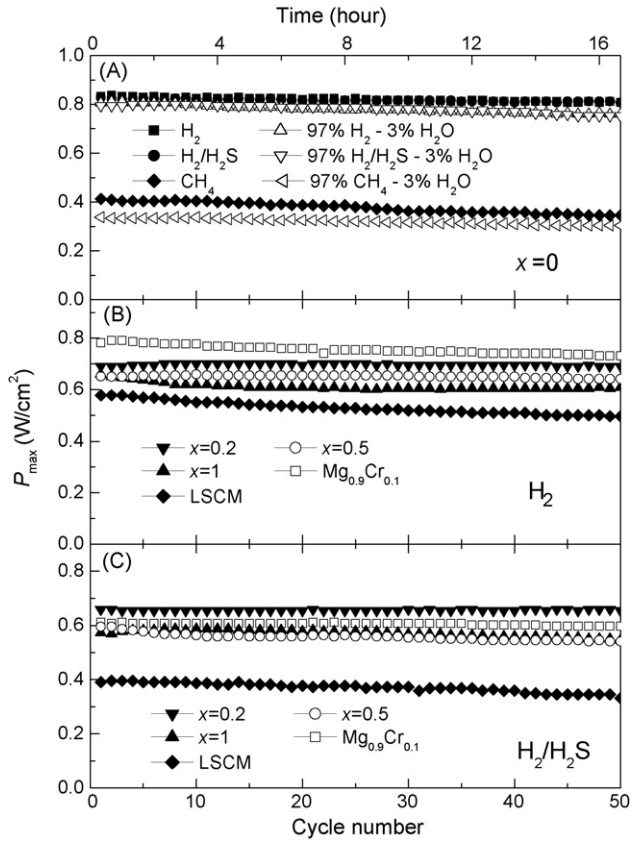

Fig. 5. The maximum power density (P_{max}) at 800 °C vs. cycle number as well as testing time for single fuel cells with various $Sr_2Mg_{1-x}Mn_xMoO_{6-\delta}$ anodes. (A) $Sr_2MgMoO_{6-\delta}$ ($x=0$) obtained in dry, wet H_2, H_2/H_2S, CH_4; (B) other anodes in dry H_2; (C) other anodes in dry H_2/H_2S. The data of $(La_{0.75}Sr_{0.25})_{0.9}Cr_{0.5}Mn_{0.5}O_{3-\delta}$ (LSCM), $Sr_2Mg_{0.9}Cr_{0.1}MoO_{6-\delta}$ anodes are also displayed for comparison.

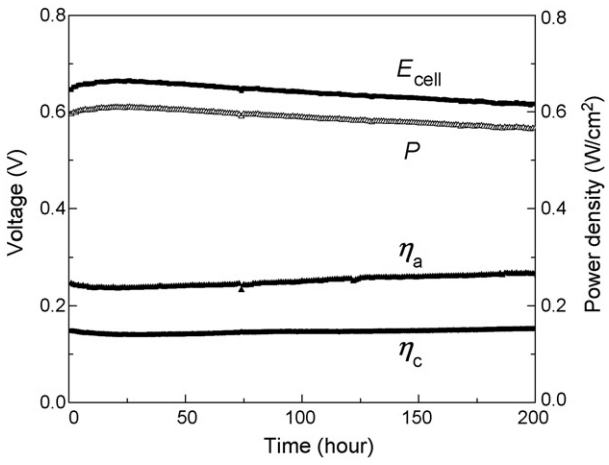

Fig. 6. The variation with time of the cell voltage, power density, cathode, anode overpotentials for $Sr_2MgMoO_{6-\delta}$ in H_2 containing 50 ppm H_2S at 800 °C. Current density was fixed at 0.92 A cm^{-2}.

signals that a commercially viable power density can be achieved with a thinner electrolyte. In dry and wet (3% H_2O) CH_4, a $P_{max} \approx 0.44$ W cm^{-2} and 0.34 W cm^{-2}, respectively, as well as its sulfur tolerance promises to enable the use of natural gas as fuel.

Fig. 5 shows P_{max} at 800 °C versus cycle number for single cells with different anodes. Whether in dry or wet fuel, $Sr_2MgMoO_{6-\delta}$ performed stably over 50 power cycles, and the curves for H_2 and H_2/H_2S essentially overlapped, indicative of the excellent tolerance for sulfur even for H_2 containing 50 ppm H_2S, see Fig. 6.

Our recent results [120] show that the La-substituted double perovskite $Sr_{2-x}La_xMgMoO_{6-\delta}$ with $0.6 \leq x \leq 0.8$ has better performance as the anode of a SOFC. With LSGM as electrolyte and $SrCo_{0.8}Fe_{0.2}O_{3-\delta}$ as cathode, the $Sr_{1.2}La_{0.8}MgMoO_{6-\delta}$ anode exhibits a P_{max} as high as 0.55 W cm^{-2} in wet CH_4 at 800 °C. It also works well in wet C_2H_6 and C_3H_8 fuels. Our experiment shows that the Mo(V)/Mo(IV) redox couple and Mg/Mo ordering play important roles in the electrochemical performance.

7. Conclusions

Present-day Ni/RDC cermets developed for a SOFC operating on syngas have been developed to where they are technically viable, but the fabrication costs are a problem. The use of natural gas as a fuel would make the technology much more competitive, but carbon formation on the anode and sulfur poisoning appear to rule out the use of Ni as a catalyst. This situation has forced the community to explore for electronically conductive oxides that are also O^{2-}-ion conductors (MIECs) in the anode atmosphere and catalytically active for fuel oxidation. The several conditions that must be met for these materials to provide the performance needed have been outlined, and some recent promising materials have been identified. Nevertheless, power densities with natural gas appear to be about half those with H_2, and the catalytic activity of these promising oxides may need to be supplemented by the impregnation of the oxides with catalysts for CH_4 oxi-

dation, a step that would increase the cost. However, the recent advances in catalytic MIEC anodes provide hope that the SOFC may become a commercially competitive option in the future mix of energy-conversion alternatives.

Acknowledgement

We thank the Robert A. Welch Foundation, Houston, TX, for support of this work.

References

[1] M. Dokiya, Solid State Ionics 152–152 (2002) 383.
[2] N.Q. Minh, Solid State Ionics 174 (2004) 271.
[3] P. Holtappels, H. Mehling, S. Roehlich, S.S. Liebermann, U. Stimming, Fuel Cells 5 (2005) 499.
[4] D.J.L. Brett, P. Aguiar, N.P. Brandon, R.N. Bull, R.C. Galloway, G.W. Hayes, K. Lillie, C. Mellors, C. Smith, A.R. Tilley, J. Power Sources 157 (2006) 782.
[5] S.C. Singhal, Solid State Ionics 135 (2000) 305.
[6] M.C. Williams, J.P. Strakey, W.A. Surdoval, J. Power Sources 143 (2005) 191.
[7] Department of Energy U.S., Fuel Cell Handbook, 7th ed., DOE, 2004.
[8] W.Z. Zhu, S.C. Deevi, Mater. Sci. Eng. A362 (2003) 228.
[9] N.P. Brandon, S. Skinner, B.C.H. Steele, Annu. Rev. Mater. Res. 33 (2003) 183.
[10] R.M. Ormerod, Chem. Soc. Rev. 32 (2003) 17.
[11] S.P. Jiang, S.H. Chan, J. Mater. Sci. 39 (2004) 4405.
[12] S. McIntosh, R.J. Gorte, Chem. Rev. 104 (2004) 4845.
[13] S.W. Tao, J.T.S. Irvine, Chem. Rec. 4 (2004) 83.
[14] A. Lashtabeg, S.J. Skinner, J. Mater. Chem. 16 (2006) 3161.
[15] T. Setoguchi, K. Okamoto, K. Eguchi, H. Arai, J. Electrochem. Soc. 139 (1992) 2875.
[16] H.S. Spacil, U.S. Patent 3,558,360, filed October 30, 1964, modified November 2, 1967, granted March 31, 1970.
[17] B. de Boer, M. Gonzalez, H.J.M. Bouwmeester, H. Verweij, Solid State Ionics 127 (2000) 269.
[18] M. Mogensen, S. Skaarup, Solid State Ionics 86–88 (1996) 1151.
[19] P. Holtappels, I.C. Vinke, L.G.J. de Haart, U. Stimming, J. Electrochem. Soc. 146 (1999) 2976.
[20] S.P. Jiang, J. Electrochem. Soc. 148 (2001) A887.
[21] S. Murakami, Y. Akiyama, N. Ishida, Y. Miyake, M. Nishioka, Y. Ttoh, T. Saito, N. Furukawa, Denki Kagaku 59 (1991) 320.
[22] S.P. Jiang, J. Electrochem. Soc. 150 (2003) E548.
[23] S. Primdahl, B.F. Sørensen, M. Mogensen, J. Am. Ceram. Soc. 83 (2000) 489.
[24] B.F. Sørensen, S. Primdahl, J. Mater. Sci. 33 (1998) 529.
[25] Y. Li, Y. Xie, J. Gong, Y. Chen, Z. Zhang, Mater. Sci. Eng. B86 (2001) 119.
[26] S. Li, R. Guo, J. Li, Y. Chen, W. Liu, Ceram. Intern. 29 (2003) 883.
[27] S.T. Aruna, M. Muthuraman, K.C. Patil, Solid State Ionics 111 (1998) 45.
[28] A. Ringuedé, J.A. Labrincha, J.R. Frade, Solid State Ionics 141–142 (2001) 549.
[29] A. Ringuedé, D. Bronine, J.R. Frade, Solid State Ionics 146 (2002) 219; A. Ringuedé, D. Bronine, J.R. Frade, Electrochim. Acta 48 (2002) 437.
[30] M. Marinšek, K. Zupan, J. Maèek, J. Power Sources 106 (2002) 178.
[31] F. Chen, M. Liu, J. Mater. Chem. 10 (2000) 2603.
[32] V. Esposito, D.Z. de Florio, F.C. Fonseca, E.N.S. Muccillo, R. Muccillo, E. Traversa, J. Eur. Ceram. Soc. 25 (2005) 2637.
[33] Y. Okawa, T. Matsumoto, T. Doi, Y. Hirata, J. Mater. Res. 17 (2002) 2266.
[34] J.W. Moon, H.L. Lee, J.D. Kim, G.D. Kim, D.A. Lee, H.W. Lee, Mater. Lett. 38 (1999) 214.
[35] T. Fukui, K. Murata, S. Ohara, H. Abe, M. Naito, K. Nogi, J. Power Sources 125 (2004) 17.
[36] Z. Ogumi, T. Ioroi, Y. Uchimoto, Z. Takehara, T. Ogawa, K. Toyama, J. Am. Ceram. Soc. 78 (1995) 593.
[37] N.M. Sammes, M.S. Brown, R. Ratnaraj, J. Mater. Sci. Lett. 13 (1994) 1124.
[38] M. Nagata, T. Esaka, H. Iwahara, Denki Kagaku 60 (1992) 792.
[39] T. Iwata, J. Electrochem. Soc. 143 (1996) 1521.
[40] D. Simwonis, F. Tietz, D. Stover, Solid State Ionics 132 (2000) 241.
[41] P. Nikolopoulos, D. Sotiropoulou, J. Mater. Sci. Lett. 6 (1987) 1429.
[42] A. Tsoga, A. Naoumidis, P. Nikolopoulos, Acta Mater. 44 (1996) 3679.
[43] R. Wilkenhoener, T. Kloidt, W. Mulléner, in: S.C. Singhal, H. Tagawa (Eds.), Proceedings of the Fifth International Symposium on Solid Oxide Fuel Cells (SOFC V), vol. 97–40, Pennington, NJ, Electrochem. Soc. (1997) 851.
[44] E. Ivers-Tiffée, A. Weber, D. Herbstritt, J. Eur. Ceram. Soc. 21 (2001) 1805.
[45] J.H. Koh, Y.S. Yoo, J.W. Park, H.C. Lim, Solid State Ionics 149 (2002) 157.
[46] R. Craciun, S. Park, R.J. Gorte, J.M. Vohs, C. Wang, W.L. Worrell, J. Electrochem. Soc. 146 (1999) 4019.
[47] J. Van Herle, R. Ihringer, A.J. McEvoy, in: S.C. Singhal, H. Taguara (Eds.), Proceedings of the Fifth International Symposium on Solid Oxide Fuel Cells (SOFC V), vol. 97–40, Pennington, NJ, Electrochem. Soc. (1997) 565.
[48] K. Ahmed, K. Foger, Catal. Today 63 (2000) 479.
[49] T. Aida, A. Abdulla, M. Ihara, H. Komiyama, K. Yamada, in: M. Dokiya, O. Yamomoto, H. Tagawa, S.C. Singhal (Eds.), Proceedings of the Fourth International Symposium on Solid Oxide Fuel Cells (SOFC IV), vol. 95–01, Pennington, NJ, Electrochem. Soc. (1995) 801.
[50] A. Abudula, M. Ihara, H. Komiyama, K. Yamada, Solid State Ionics 86–88 (1996) 1203.
[51] E.P. Murray, T. Tsai, S.A. Barnett, Nature 400 (1999) 649.
[52] S. Park, R. Craciun, J.M. Vohs, R.J. Gorte, J. Electrochem. Soc. 146 (1999) 3603.
[53] J. Liu, B.D. Madsen, Z.Q. Ji, S.A. Barnett, Electrochem. Solid State Lett. 5 (2002) A122.
[54] J. Liu, S.A. Barnett, Solid State Ionics 158 (2003) 11.
[55] Y. Lin, Z. Zhan, J. Liu, S.A. Barnett, Solid State Ionics 176 (2005) 1827.
[56] C. Xia, F. Chen, M. Liu, Electrochem. Solid State Lett. 4 (2001) A52.
[57] Y. Lin, Z. Zhan, S.A. Barnett, J. Power Sources 158 (2006) 1313.
[58] Z. Zhan, Y. Lin, M. Pillai, I. Kim, S.A. Barnett, J. Power Sources 161 (2006) 460.
[59] Y. Matsuzaki, I. Yasuta, Solid State Ionics 132 (2000) 261.
[60] M. Weston, I.S. Metcalfe, Solid State Ionics 113–115 (1998) 247.
[61] P. Vernoux, M. Guillodo, J. Fouletier, A. Hammou, Solid State Ionics 135 (2000) 425.
[62] H. Uchida, M. Sugimoto, M. Watanabe, in: H. Yokokawa, S.C. Singhal (Eds.), Proceedings of the Seventh International Symposium on Solid Oxide Fuel Cells (SOFC VII), Tsukuba, Ibaraki, Japan, 2001, p. 653.
[63] S. Hui, A. Petric, J. Eur. Ceram. Soc. 22 (2002) 1673.
[64] A. Bieberle, L.J. Gauckler, Z. Metallkd. 92 (2001) 796.
[65] S.P. Jiang, Y.Y. Duan, J.G. Love, J. Electrochem. Soc. 149 (2002) A1175.
[66] D. Hirabayashi, A. Tomita, M.E. Brito, T. Hibino, U. Harada, M. Nagao, M. Sano, Solid State Ionics 168 (2004) 23.
[67] S.A. Barnett, Handbook of Fuel Cell Technology, vol. 4, Wiley, Hoboken, NJ, 2003, p. 98.
[68] O.A. Marina, C. Bagger, S. Primdahl, M. Mogensen, Solid State Ionics 123 (1999) 199.
[69] S.J.A. Livermore, J.W. Cotton, R.M. Ormerod, J. Power Sources 86 (2000) 411.
[70] T. Hibino, A. Hashimoto, K. Asano, M. Yano, M. Suzuki, M. Sano, Electrochem. Solid State Lett. 5 (2002) A242.
[71] T. Hibino, A. Hashimoto, M. Yano, M. Suzuki, S. Yoshida, M. Sano, J. Electrochem. Soc. 149 (2002) A133.
[72] A. Tsoga, A. Gupta, A. Naoumidis, D. Skarmoutsos, P. Nikolopoulos, Ionics 4 (1999) 234.
[73] A. Tsoga, A. Naoumidis, A. Gupta, D. Stover, Mater. Sci. Forum 308–311 (1999) 234.

[74] A. Tsoga, A. Gupta, A. Naoumidis, P. Nikolopoulos, Acta Mater. 48 (2000) 4709.
[75] K. Huang, R. Tichy, J.B. Goodenough, C. Milliken, J. Am. Ceram. Soc. 81 (1998) 2581.
[76] K. Huang, J.-H. Wan, J.B. Goodenough, J. Electrochem. Soc. 148 (2001) A788.
[77] J.H. Wan, J.Q. Yan, J.B. Goodenough, J. Electrochem. Soc. 152 (2005) A1511.
[78] S.M. Choi, K.T. Lee, S. Kim, M.C. Chun, H.L. Lee, Solid State Ionics 131 (2000) 221.
[79] X. Zhang, S. Ohara, H. Okawa, R. Maric, T. Fukui, Solid State Ionics 139 (2001) 145.
[80] K. Zheng, B.C.H. Steele, M. Sahibzada, I.S. Metcalfe, Solid State Ionics 86–88 (1996) 1241.
[81] B.C.H. Steele, Solid State Ionics 129 (2000) 95.
[82] S. Zha, A. Moore, H. Abernathy, M. Liu, J. Electrochem. Soc. 151 (2004) A1128.
[83] O. Costa-Nunes, R.J. Gorte, J.M. Vohs, J. Power Sources 141 (2005) 241.
[84] H. Kim, S. Park, J.M. Vohs, R.J. Gorte, J. Electrochem. Soc. 148 (2001) A693.
[85] C. Lu, W.L. Worrell, J.M. Vohs, R.J. Gorte, J. Electrochem. Soc. 150 (2003) A1357.
[86] R.J. Gorte, J.M. Vohs, C. Wang, Adv. Mater. 12 (2000) 1465.
[87] J.M. Vohs, S. Park, R.J. Gorte, Nature 404 (2000) 265.
[88] H.P. He, J.M. Vohs, R.J. Gorte, J. Electrochem. Soc. 150 (2003) A1470.
[89] S.W. Jung, C. Lu, H.P. He, K.Y. Ahn, R.J. Gorte, J.M. Vohs, J. Power Sources 154 (2006) 42.
[90] S. McIntosh, J.M. Vohs, R.J. Gorte, Electrochim. Acta 47 (2002) 3815.
[91] E.S. Putna, J. Stubenrauch, J.M. Vohs, R.J. Gorte, Langmuir 11 (1995) 4832.
[92] H. Kim, C. Lu, W.L. Worrell, J.M. Vohs, R.J. Gorte, J. Electrochem. Soc. 149 (2002) A247.
[93] Z. Xie, W. Zhu, B. Zhu, C. Xia, Electrochim. Acta 51 (2006) 3052.
[94] H.P. He, R.J. Gorte, J.M. Vohs, Eletrochem, Solid State Lett. 8 (2005) A279.
[95] T. Baidya, A. Gayen, M.S. Hegde, N. Ravishankar, L. Dupont, J. Phys. Chem. B110 (2006) 5262.
[96] F. Chen, M. Liu, J. Solid State Electrochem. 3 (1998) 7.
[97] Q. Fu, X. Xu, D. Peng, X. Liu, G. Meng, J. Mater. Sci. 38 (2003) 2901.
[98] N. Maffei, G. de Silveira, Solid State Ionics 159 (2003) 209.
[99] M.F. Hsu, L.J. Wu, J.M. Wu, Y.H. Shiu, K.F. Lin, Electrochem. Solid State Lett. 9 (2006) A193.
[100] O. Yamamoto, Y. Takeda, R. Kanno, M. Noda, Solid State Ionics 22 (1987) 241.
[101] S.W. Tao, J.T.S. Irvine, J. Electrochem. Soc. 151 (2004) A252.
[102] S.W. Tao, J.T.S. Irvine, Nat. Mater. 2 (2003) 320.
[103] S.W. Tao, J.T.S. Irvine, J.A. Kilner, Adv. Mater. 17 (2005) 1734.
[104] J.H. Wan, J.H. Zhu, J.B. Goodenough, Solid State Ionics 177 (2006) 1211.
[105] L. Aguilar, S. Zha, S. Li, J. Winnick, M. Liu, Electrochem. Solid State Lett. 7 (2004) A324.
[106] S. Zha, Z. Cheng, M. Liu, Electrochem. Solid State Lett. 8 (2005) A406.
[107] J. Canales-Vásquez, S.W. Tao, J.T.S. Irvine, Solid State Ionics 159 (2003) 159.
[108] O.A. Marina, N.L. Canfield, J.W. Stevenson, Solid State Ionics 149 (2002) 21.
[109] R. Mukundan, E.L. Brosha, F.H. Garzon, Electrochem. Solid State Lett. 7 (2004) A5.
[110] J. Canles-Vásquez, J.C. Ruiz-Morales, J.T.S. Irvine, W. Zhou, J. Electrochem. Soc. 152 (2005) 1458.
[111] J.C. Ruiz-Morales, J. Canales-Vásquez, C. Savaniu, D. Marrero-López, W. Zhou, J.T.S. Irvine, Nature 439 (2006) 568.
[112] Q.X. Fu, F. Tietz, D. Stöver, J. Electrochem. Soc. 153 (2006) D74.
[113] V. Vashook, J. Zosel, R. Müller, P. Shuk, L. Vasylechko, H. Ullmann, U. Guth, Fuel Cells 6 (2006) 293.
[114] A.L. Sauvet, J. Fouletier, F. Gaillard, M. Primet, J. Catal. 209 (2002) 25.
[115] J. Lindén, T. Yamamoto, M. Karppinen, H. Yamauchi, T. Pietari, Appl. Phys. Lett. 76 (2000) 2925.
[116] Cz. Kapusta, P.C. Riedi, D. Zajac, M. Sikora, J.M. De Teresa, L. Morellon, M.R. Ibarra, J. Magn. Magn. Mater. 242–245 (2002) 701.
[117] J.B. Goodenough, Solid State Ionics 26 (1988) 87.
[118] Y.H. Huang, R.I. Dass, J.C. Denyszyn, J.B. Goodenough, J. Electrochem. Soc. 153 (2006) A1266.
[119] Y.H. Huang, R.I. Dass, Z.L. Xing, J.B. Goodenough, Science 312 (2006) 254.
[120] Y. Ji, Y.H. Huang, J.R. Ying, J.B. Goodenough, Electrochem. Commun. 9 (2007) 1881.